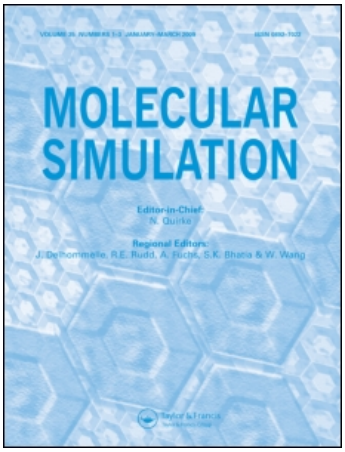

Molecular Simulation
Publication details, including instructions for authors and subscription information:
http://www.informaworld.com/smpp/title~content=t713644482

A nonorthogonal tight-binding model for hydrocarbon molecules and nanostructures

J. Zhao[a]; X. Guo[b]; B. Wen[c]
[a] State Key Laboratory of Materials Modification by Laser, Electron, and Ion Beams & College of Advanced Science and Technology, Dalian University of Technology, Dalian, People's Republic of China [b] Department of Engineering Mechanics and State Key Laboratory of Structural Analysis for Industrial Equipment, Dalian University of Technology, Dalian, People's Republic of China [c] Department of Materials Engineering, Dalian University of Technology, Dalian, People's Republic of China

To cite this Article Zhao, J. , Guo, X. and Wen, B.(2007) 'A nonorthogonal tight-binding model for hydrocarbon molecules and nanostructures', Molecular Simulation, 33: 8, 703 — 709
To link to this Article: DOI: 10.1080/08927020701203706
URL: http://dx.doi.org/10.1080/08927020701203706

Molecular Simulation, Vol. 33, No. 8, July 2007, 703–709

Taylor & Francis
Taylor & Francis Group

A nonorthogonal tight-binding model for hydrocarbon molecules and nanostructures

J. ZHAO†*, X. GUO‡ and B. WEN¶§

†State Key Laboratory of Materials Modification by Laser, Electron, and Ion Beams & College of Advanced Science and Technology, Dalian University of Technology, Dalian 116024, People's Republic of China
‡Department of Engineering Mechanics and State Key Laboratory of Structural Analysis for Industrial Equipment, Dalian University of Technology, Dalian 116024, People's Republic of China
¶Department of Materials Engineering, Dalian University of Technology, Dalian 116024, People's Republic of China

(Received January 2006; in final form June 2006)

In spirit of extended-Hückel approximations, we have developed a nonorthogonal tight-binding total energy model for hydrocarbons with only a few adjustable parameters. Our model reproduces the geometry structures, binding energies, on-site charge transfer and vibrational frequencies of a variety of hydrocarbon molecules reasonably well. Comparative calculations on carbon fullerenes and nanotubes using tight-binding model and density functional theory demonstrate the potential of applying this model to large scale simulations of carbon nanostructures.

Keywords: Tight-binding; Hydrocarbon; Carbon nanostructures; Binding energy

1. Introduction

In recent years, there have been tremendous progress in the atomistic simulations of materials using the state-of-the-art modern computers [1]. These simulation methods can be roughly divided into two classes: classical-based (e.g. pair potentials, embedded-atom potentials, bond order potentials, force field, etc.) and quantum-based (e.g. *ab initio* Car-Parrinello method, tight-binding molecular dynamics, etc.). In either classes, a total energy model describing the interatomic interaction in the materials is essential to conduct the atomistic simulations. Among those existing total energy methods, quantum *ab initio* approaches based on first-principles *electronic structure* calculations are highly accurate but require significant amount of CPU time [1,2]. On the other hand, empirical potentials such as universal force field [3], bond order potentials [4,5] are very fast, but their application is somewhat limited due to the total neglect of electrons. Between these two sides, tight-binding total energy method constitutes a reasonable compromise of (fast) empirical potentials and (accurate) *ab initio* methods. Within the tight-binding approaches, the system is still described in a quantum-mechanical manner, while the computational cost is significantly reduced by the parameterized Hamiltonian and the minimum set of valence orbitals. The computational efficiency of the tight-binding simulations can be further improved to be linear scale of the system size N if the order-N algorithm is used [6,7].

In 1979, Chadi has introduced the first tight-binding total energy model [8] by adding a two-body repulsive term into the tight-binding electronic Hamiltonian. In this way, the Slater–Koster tight-binding approach [9] was generalized into a total energy model for silicon. During the past 25 years, plenty of tight-binding total energy models have been developed for a variety of materials [10–18]. Usually, there is a number of adjustable parameters in these models fitted from experimental data or *ab initio* calculations. In general, the transferability of the model depend on the physical picture and approximation of the model as well as the choice of "training set" as input datain the fitting procedure.

Instead of including a large number of empirical parameters and employing a huge training set, here we develop an universal scheme of constructing minimal-parameter nonorthogonal tight-binding model with only a small set of adjustable parameters. In our method,

*Corresponding author. Email: zhaojj@dlut.edu.cn
§Email: wenbin@dlut.edu.cn

Molecular Simulation
ISSN 0892-7022 print/ISSN 1029-0435 online © 2007 Taylor & Francis
http://www.tandf.co.uk/journals
DOI: 10.1080/08927020701203706

the overlap integrals are computed exactly from the Slater-type atomic orbitals, while the Hamiltonian matrix elements are obtained from the overlap integrals using extended Hückel approximation. A simple analytic repulsive potential is included to describe the total energy of systems. In this work, we fit the model parameters for hydrocarbons and tested this model for a variety of molecules. In particular, the validity of the present extended Hückel based tight-binding (EHTB) model in the carbon nanostructures such as fullerenes and nanotubes are examined by comparing with the first-principles calculations employing all-electron density functional theory. The satisfactory performance of the EHTB model indicates potential applications in large scale simulations of the carbon nanostructures.

2. Model and parameters

In a tight-binding total energy model, the binding energy of a molecule consists of the electronic binding energy $E_{\rm el}$ and ionic repulsive energy $E_{\rm rep}$. The electronic binding energy $E_{\rm el}$ is calculated from summation of one-electron energies ϵ_k for occupied states, where the electron eigenvalues ϵ_k are determined by the secular equation:

$$\det|H_{ij} - \epsilon S_{ij}| = 0. \tag{1}$$

Within extended Hückel approximation [19], the Hamiltonian matrix elements H_{ij} are calculated from overlap matrix elements S_{ij} of valence orbitals

$$H_{ij} = \frac{K}{2} S_{ij}(H_{ii} + H_{jj}). \tag{2}$$

In equation (2), the overlap integrals S_{ij} are evaluated using atomic Slater orbital parameters ζ taken from [22] (table 1) and restored in numerical tables read by the program. In this work, we adopt an exponential distance-dependent function of the "extended Hückel constant" K as proposed by Calzaferri *et al.* [20].

$$K(r) = 1 + k_0 \mathrm{e}^{-\delta(r-r_0)} \tag{3}$$

In Ref. [20], it was shown that the repulsive interaction between atomic cores can be evaluated analytically if the Slater-type function is used for the atomic orbitals. In a previous work, a combination of exponential repulsive function and extended Hückel Hamiltonian was developed by Curotto *et al.* for nickel clusters [21]. Such pair-wise exponential function was also widely used in the nonorthogonal tight-binding total energy models of semiconductors like germanium [13]. In this work, we express the repulsive interaction by an exponential function as interatomic distance, i.e.

$$E_{\rm rep} = \sum_{ij} \phi_0 \mathrm{e}^{-\beta(r-r_0)} \tag{4}$$

In our EHTB model, there are five adjustable parameters, r_0, k_0, δ, ϕ_0, β, for each pair of atoms (H—H, C—H, C—C). In practice, we fit the parameters to reproduce the experimental binding energy and the *ab initio* binding curve from DFT calculations for the small molecules like H_2, CH_4 and C_2H_6. The obtained parameters are given in table 1.

Table 1. Parameters of EHTB model for C, H atoms developed in this work.

Element	*n*	ζ_s	H_{ss} *(eV)*	ζ_p	H_{pp} *(eV)*
H	1	1.30	−11.57		
C	2	1.71	−19.38	1.625	−11.07
	r_0 (Å)	k_0	δ (1/Å)	ϕ_0 (eV)	β (1/Å)
H—H	0.75	0.653	0.60	1.36	5.59
C—H	1.10	0.771	0.55	1.26	5.17
C—C	1.26	0.920	0.46	2.85	5.21

n is the principal quantum number. The atomic Slater orbital coefficients for *s* orbital (ζ_s) and *p* orbital (ζ_p) are taken from Ref. [22]. The atomic orbital energies H_{ij} are adjusted from the original atomic values in Ref. [23] to improve overall performance of our model. Other parameters (r_0, k_0, δ, ϕ_0, β) for each pair of atoms (C—C, C—H, H—H) are fitted from experimental binding energy and the *ab initio* binding curve for H_2, CH_4, C_2H_6 molecules.

3. Hydrocarbon molecules

Using the EHTB model developed in this work, we have tested a variety of organic hydrocarbon molecules and radicals. The geometry optimizations were performed using a limited memory Broyden–Fletcher–Goldfarb–Shanno algorithm [24]. As the simplest cases, we calculate the equilibrium geometries and binding energies of the small hydrocarbons such as CH, CH_2 (methylene, singlet state), CH_3 (methyl), CH_4 (methane), C_2H_2 (acetylene), C_2H_4 (ethylene), C_2H_6 (ethane), C_3H_6 (cyclopropane), C_4H_6 (1,3-butadiene), $C(CH_3)_4$ (neopentane), C_6H_6 (benzene) and C_8H_8 (cubane). In table 2, we compare the geometry parameters for those molecules from our EHTB calculations with the measured numbers [25–27]. Overall speaking, the EHTB model describes the geometry structures of these hydrocarbons with different C—C bonding characteristics such as single, double, triple and resonant bonds reasonably well. Amongthose molecules, the C—C bond lengths of the single bonds and resonance bonds by EHTB model are rather close to experiments, while the EHTB model tends to underestimate the length of C—C double and triple bonds.

We further examine the performance of the EHTB model by applying it to a wider range of hydrocarbon molecules, which were previously considered in Ref. [5] by Brenner. Table 3 compares the theoretical binding energy by EHTB model and the experimental data collected by Brenner [5]. One can see very good overall agreement, especially considering the simplicity of the formulism and the small number of adjustable parameters of our model. Careful comparisons reveal that the average error for binding energy is 1.31% for alkanes, 1.98% for alkenes, 8% for alkynes, 0.94% for aromatics and 2.8% for radicals. Therefore, we conclude that the binding energy

Table 2. Geometrical variables (A—B: bond length in unit of Å, A—B—C: bond angle in unit of degree) for small hydrocarbons molecules from EHTB and experiments.

Molecule		*Variable*	*EHTB*	*Experiment*
H_2		H—H	0.76	0.74
CH		C—H	1.10	1.12
CH_2	Methylene	C—H	1.09	1.08
		H—C—H	113.1	136.0
CH_3	Methyl	C—H	1.08	1.08
CH_4	Methane	C—H	1.09	1.09
C_2H_2	Acetylene	C—C	1.15	1.20
		C—H	1.07	1.06
C_2H_4	Ethylene	C—C	1.28	1.33
		C—H	1.10	1.08
		H—C—C	123.5	100.9
C_2H_6	Ethane	C—C	1.53	1.53
		C—H	1.09	1.09
C_3H_6	Cyclopropane	C—C	1.53	1.51
		C—H	1.08	1.09
C_4H_6	1,3-Butadiene	C1—C2	1.29	1.34
		C2—C3	1.52	1.47
		C—C—C	126.2	122.9
C_4H_{10}	*n*-Butane	C1—C2	1.54	1.53
		C2—C3	1.55	1.53
		C—C—C	112.2	112.8
$CH(CH_3)_3$	Isobutane	C—C	1.55	1.54
$C(CH_3)_4$	Neopentane	C—C	1.55	1.54
		C—H	1.09	1.12
		H—C—C	109.4	110.0
C_6H_6	Benzene	C—C	1.39	1.40
		C—H	1.09	1.09
C_8H_8	Cubane	C—C	1.63	1.58
		C—H	1.07	1.10

Most experimental data are taken from Ref. [25], expect CH_2 from Ref. [26] and C_8H_8 from Ref. [27].

predicted by EHTB is reasonably accurate except for alkyne-type molecules.

Using the EHTB model, we have studied the vibrational properties of several small hydrocarbon molecules (H_2, CH_4, C_2H_2, C_2H_4, C_2H_6) by applying finite displacement to each atom. The theoretical vibrational frequencies are compared with experimental data in table 4. For those CH stretch modes, the discrepancy between theoretical and experimental frequencies are within $100\,cm^{-1}$ or $\sim 3\%$. For some low-frequency modes, the discrepancy can be larger, while the overall agreement is still acceptable. Thus, the EHTB model can be used to give a rough description for the vibration properties of hydrocarbon molecules. Furthermore, the vibrational frequencies are important characteristics for the chemical bonding of molecules. The agreement between theory and experiments further demonstrates the validity of the EHTB model.

In addition to the structural, bonding and vibrational properties, we find that the present EHTB model is also able to describe the internal electron transfer in the hydrocarbon molecules. In table 5, we present the on-site charge transfer of C and H atoms for several hydrocarbon molecules from EHTB calculations and from Mulliken charge analysis by Hartree–Fock theory calculations with MP2 correction implemented in a GAMESS program [28]. For all the molecules studied, the agreement between EHTB and HF-MP2 results are quite good.

4. Carbon nanostructures

One major motivation for developing the present semiempirical total energy model is to simulate carbon nanostructures up to large scale with acceptable accuracy. In this work, we apply the EHTB model to carbon fullerenes and nanotubes up to about 200 atoms. To check the performance of the EHTB model, we carried out comparative all-electron DFT computations using a DMol package [29]. In the DFT calculations, we used a double numerical (DN) basis set and the PW91 exchange-correlation functional within generalized gradient approximation (GGA) [30].

To examine the performance of EHTB model on fullerene of different size, we have studied several representative carbon fullerenes from C_{20} to C_{84} [37,38]. The EHTB and GGA binding energies as function of fullerene size are plotted in figure 1. The increase of binding energy with the fullerene size from EHTB and GGA calculations are very close. We found that our EHTB optimization lead to Jahn–Teller distortion for small fullerenes [37] like C_{20} and C_{24}, which can reduce their symmetry from the higher I_h and D_{6h} ones to lower D_3 and D_6, respectively. On the other hand, it is worthy to note that our EHTB is not able to consider the high-spin states as the first-principles DFT. In fact, the ground state of C_{28} (T_d) is a quintet and the ground state of C_{36} (D_{6h}) is a triplet at GGA level [37].

Moreover, it is more critical to validate the performance of the EHTB model by computing the relative energies of the relative energies between isomers of a specific fullerene with given size. In previous studies, it was shown that both the semiempirical quantum chemistry methods (like MNDO, AM1, PM3) [39] and the density functional tight binding (DFTB) [40] can reasonably reproduce the *ab initio* results at B3LYP/6-31G* level. Table 6 presents the relative energies of fullerene isomers for several sizes (C_{30}, C_{32}, C_{34}, C_{36}, C_{40}, C_{84}) from *ab initio* B3LYP [39], semiemprical AM1 and PM3 [39] and EHTB calculations. It is clearly shown that the performance of EHTB model is comparable to the well-established semiempirical methods like AM1 and PM3 for all the sizes studied.

Similar to the discussion of fullerenes in figure 1, we have also studied the binding energies of carbon nanotubes as function of nanotube diameter. Nanotubes of different diameters, from (5,5) to (10,10) tubes, were considered. We adopted the finite tube model with three unit cells of armchair nanotubes and used hydrogen termination on the two ends. The binding energies per carbon atom as function of inverse of tube diameter ($1/D$) from EHTB and GGA calculations are compared in figure 2, which show close agreement. Both EHTB and GGA results indicate a linear dependence of binding energy vs. $1/D$, which can be understood by the elastic strain energy of a single graphene sheet [31].

We constructed larger finite tube models to study carbon nanotubes with topological defects on the sidewall. We built a finite (6,6) tube with 15 layers (7.5 unit cell)

Table 3. Binding energy (eV) for a variety of small hydrocarbon molecules and radicals from EHTB model and experiments.

Molecule		*Formula*	*EHTB (eV)*	*Experiment (eV)*
Alkanes	Methane	CH_4	17.6	17.6
	Ethane	C_2H_6	29.7	29.7
	Propane	C_3H_8	41.8	42.0
	n-Butane	C_4H_{10}	53.8	54.3
	n-Pentane	C_5H_{12}	65.9	66.6
	Cyclopropane	C_3H_6	34.8	35.8
	Cyclobutane	C_4H_8	46.9	48.2
	Cyclopentane	C_5H_{10}	60.1	61.4
	Cyclohexane	C_6H_{12}	72.3	73.6
Alkenes	Ethylene	C_2H_4	24.4	23.6
	Allene	C_3H_4	31.3	29.6
	But-1,3-diene	C_4H_6	43.4	42.6
	1-Butene	C_4H_8	48.6	48.5
	Cis-butene	C_4H_8	48.6	48.6
	Cyclopropene	C_3H_4	28.5	28.8
	Cyclobutene	C_4H_6	41.0	42.4
	Cyclopentene	C_5H_8	54.7	55.6
	2,3-Dimethylbut-2-ene	C_6H_{12}	72.5	73.4
Alkynes	Acetylene	C_2H_2	19.8	17.1
	Propyne	C_3H_6	31.9	29.7
	1-Butyne	C_4H_6	43.9	42.0
	2-Butyne	C_4H_6	44.0	42.2
Aromatics	Benzene	C_6H_6	57.5	57.5
	Toluene	C_7H_8	69.5	70.1
	Ethylbenzene	C_8H_{10}	81.6	82.5
	Ethenylbenzene	C_8H_8	76.4	76.5
	Ethynylbenzene	C_8H_8	71.7	69.9
	Naphthalene	$C_{10}H_8$	90.2	91.2
Radicals		CH_2	8.1	7.8
		CH_3	12.8	12.7
		$H_3C_2H_2$	25.1	25.5
		H_2C_2H	19.9	18.9
		C_2H	12.8	12.2
	Phenyl	C_6H_5	52.5	52.7

and applied hydrogen termination on the two ends, which contains 180 C atoms and 24 H atom. Topological defects such as seven-member ring, eight-member ring [32] were then created in the center of the finite tube. Full geometry optimization at both EHTB and GGA level were performed to compute the formation energy of the topological defects. For the finite (6,6) tube without sidewall defects, the C—C bond length in the central unit cell by EHTB model is 1.46 and 1.43 Å, respectively, rather close to GGA bond length of 1.44 and 1.43 Å. Formation energy of a Stone–Wales defect with two seven-member rings and two five-member rings on a finite (6,6) tube is 2.78 eV from EHTB model, very close to the GGA result (2.75 eV). For the defect with eight-member ring, the formation energy predicted by our EHTB model is 4.56 eV, while it is 5.11 eV from GGA calculations.

One potential application of our EHTB model is to conduct molecular dynamics simulation on the mechanical response of different carbon nanotubes under external mechanical loading. Young's modulus is the essential quantity for describing the elastical response of a nanotube. We constructed hydrogen-terminated (5,5) and (9,0) finite nanotube models with eight and four unit cells (160 and 144 carbon atoms), respectively. To compute the Young's modulus, we applied uniform axial elongation on the equilibrium tube length up to 1%. The Young's modulus (Y) calculated from our EHTB model are 0.91 TPa for (9,0) tube and 0.96 TPa for (5,5) tube. There have been a number of previous theoretical calculations on the Young's modulus of single-walled carbon nanotube and most of the results are around 1 TPa [33]. For example, a previous all-electron *ab initio* calculations at Hartree–Fock 6-31G* level [34] predicted $Y = 1.14$ TPa for (9,0) tube and $Y = 1.06$ TPa for (5,5) tube. Our EHTB results agree well with those previous calculations [33,34]. Therefore, it could be employed in the simulation of the mechanical properties of carbon nanotubes.

Our EHTB model might also be useful to the simulation of nanotube chemistry. As a specific example, we studied covalent sidewall functionalization of carbon nanotubes by a CH_2 group. A finite (6,6) tube with 4.5 unit cells and hydrogen termination ontwo ends was used. The atomic structure and the associated geometry parameters of the CH_2 attached tube are shown in figure 3 and table 7, respectively. Both EHTB and GGA calculations have predicted the opening of nanotube sidewall by functionalization, in agreement with a recent *ab initio studies* [35,36]. As shown in table 7, geometry parameters from EHTB method agree well with GGA results. In particular, the distance between two C atoms (C2—C3 in table 7) attached to the CH_2 addend on the nine-layered (6,6) tube is 2.28 Å from EHTB calculation and is 2.13 Å from GGA

Table 4. Vibration frequencies (in unit of cm^{-1} and associated modes for small hydrocarbon molecules from EHTB calculations and experiments [26].

Molecule	*Mode*	*EHTB*	*Experiment*
H_2	HH stretch	4497	4160
CH_4	*d*-Stretch	3091	3019
	s-Stretch	3051	2917
	d-Deform	1401	1534
	d-Deform	1252	1306
C_2H_2	CH stretch	3327	3374
	CH stretch	3306	3289
	CC stretch	2231	1974
	CH bend	887	730
	CH bend	667	612
C_2H_4	CH_2 *a*-stretch	3144	3106
	CH_2 *a*-stretch	3096	3103
	CH_2 *s*-stretch	3062	3026
	CH_2 *s*-stretch	3055	2989
	CC stretch	1681	1623
	CH_2 scissors	1352	1444
	CH_2 scissors	1271	1342
	CH_2 rock	1187	1236
	CH_2 twist	1038	1023
	CH_2 wag	996	949
	CH_2 wag	921	943
	CH_2 rock	670	826
C_2H_6	CH_3 *s*-stretch	3067	2986
	CH_3 *d*-stretch	3003	2985
	CH_3 *d*-stretch	2984	2969
	CH_3 *s*-stretch	2978	2954
	CH_3 *d*-deform	1372	1469
	CH_3 *d*-deform	1348	1468
	CH_3 *s*-deform	1340	1388
	CH_3 *s*-deform	1333	1379
	CH_3 rock	1205	1190
	CC stretch	1171	995
	CH_3 rock	839	822

calculations, respectively, while the *ab initio* calculations in Ref. [35] gave a 2.23 Å C—C distance for a finite nine-layered (5,5) tube. It is noteworthy that the quantum/empirical hybrid approach like ONIOM cannot reproduce such sidewall opening [35], although it has been widely used in the computational study of carbon nanotubes.

The successes of the series of calculations above indicate that the EHTB method developed in this work can be applicable to the carbon fullerenes and nanotubes in many aspects, such as binding energies, mechanical properties, structural defects, chemical functionalization, etc. Our works on these directions are underway.

Table 5. On-site Mulliken charge (in unit of $|e|$ of carbon (Q_C) and hydrogen (Q_H) atoms from ETTB model compared with HF-MP2 calculations (numbers in parentheses). The electron transfer from hydrogen to carbon are well reproduced.

	Q_C	Q_H
Methane (CH_4)	−0.5408 (−0.6616)	0.1352 (0.1654)
Ethyne (C_2H_2)	−0.2526 (−0.2296)	0.2526 (0.2296)
Ethene (C_2H_4)	−0.3148 (−0.2946)	0.1574 (0.1473)
Ethane (C_2H_6)	−0.3945 (−0.4893)	0.1315 (0.1631)
Benzene (C_6H_6)	−0.1454 (−0.1452)	0.1454 (0.1452)
Naphthalene ($C_{10}H_8$)	−0.1453 (−0.1439)	0.1408 (0.1411)
	−0.1375 (−0.1438)	0.1513 (0.1489)
	−0.0185 (−0.0046)	

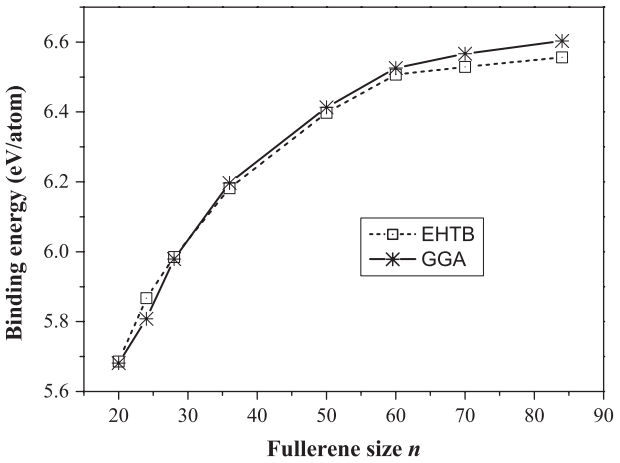

Figure 1. Binding energy of carbon fullerenes from EHTB and density functional GGA calculations. Some representative fullerenes with high symmetry are considered, such as C_{20} (D_3), C_{24} (D_6), C_{28} (T_d), C_{36} (D_{6h}), C_{50} (D_{5h}), C_{60} (I_h), C_{70} (D_{5h}), C_{84} (D_{2d}). In order to compare the size-dependence of the two methods, a systematic shift of −0.79 eV was applied to the GGA binding energy. Excellent agreement in the size dependent trend can be seen.

Table 6. Relative energies (kcal/mol) of small fullerenes at B3LYP/6-31G*, semiempirical quantum chemistry methods, i.e. AM1, PM3 and EHTB model. The B3LYP, AM1 and PM3 results are taken from previous calculations by Chen and Thiel [39].

Fullerene isomers	*Symmetry*	*B3LYP*	*EHTB*	*AM1*	*PM3*
C30_1	C_{2v}	55.6	62.0	72.8	63.8
C30_1	C_{2v}	4.0	9.4	26.6	23.0
C30_1	C_{2v}	0.0	0.0	0.0	0.0
C32_1	C_2	60.3	49.3	61.8	56.4
C32_2	D_2	65.5	62.3	61.5	54.6
C32_3	D_{3d}	73.9	163.1	99.1	91.2
C32_4	C_2	26.0	26.8	27.0	24.2
C32_5	D_{3h}	78.3	77.4	81.6	72.0
C32_6	D_3	0.0	0.0	0.0	0.0
C34_1	C_2	66.3	64.5	67.8	54.1
C34_2	C_s	25.0	29.5	21.5	13.3
C34_3	C_s	21.3	25.1	33.3	16.6
C34_4	C_2	5.8	9.4	−3.4	−10.6
C34_5	C_2	0.0	0.0	0.0	0.0
C34_6	C_1	25.5	31.0	32.4	22.5
C36_1	C_2	80.5	68.6	84.0	74.8
C36_2	D_2	110.6	112.6	145.0	129.8
C36_3	C_1	60.2	58.0	70.6	62.3
C36_4	C_s	78.2	82.2	105.1	93.6
C36_5	D_2	91.1	101.2	135.6	120.9
C36_6	D_{2d}	32.4	21.9	27.6	23.6
C36_7	C_1	37.8	35.1	42.7	37.4
C36_8	C_s	24.7	29.6	38.6	33.6
C36_9	C_{2v}	7.4	20.3	8.7	6.5
C36_10	C_2	48.3	52.5	66.7	60.2
C36_11	C_2	13.4	18.5	33.8	30.6
C36_12	C_2	17.9	13.4	41.0	37.9
C36_13	D_{3h}	40.7	54.3	71.2	62.8
C36_14	D_{2d}	0.0	0.0	0.0	0.0
C36_15	D_{6h}	3.3	10.5	24.3	30.0
C40_38	D_2	0.0	0.0	0.0	0.0
C40_39	D_{5d}	10.6	7.8	9.7	8.8
C84_20	T_d	30.8	21.1	30.3	25.3
C84_21	D_2	16.4	15.4	19.2	19.0
C84_22	D_2	0.4	0.1	0.4	0.5
C84_23	D_{3d}	0.0	0.0	0.0	0.0
C84_24	D_{6h}	7.2	5.8	8.1	6.8

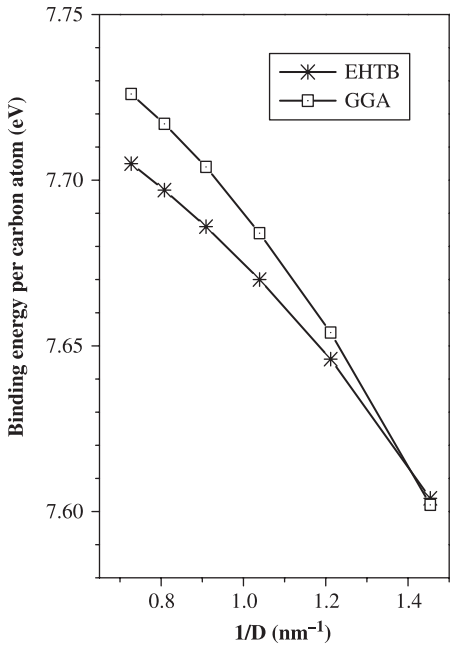

Figure 2. Binding energy per carbon atom of carbon nanotubes with different diameters (D) from EHTB and GGA calculations. Armchair nanotubes from (5,5) tube of $D = 0.69$ nm to (10,10) tube of $D = 1.38$ nm were included. In order to compare the diameter dependence of the two methods, a systematic shift of -0.7 eV was applied to the GGA results.

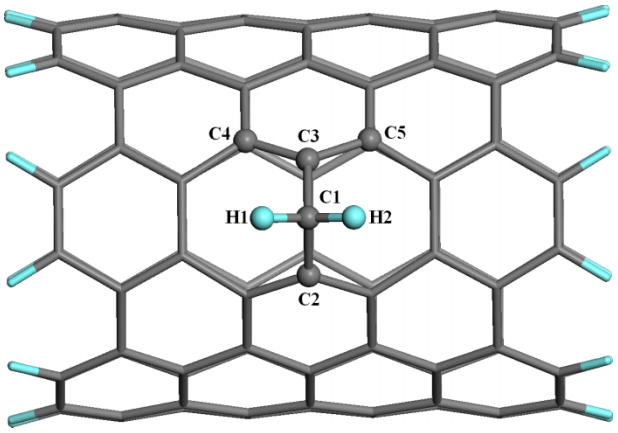

Figure 3. Atomic structure of a CH_2 group attached to a finite (6,6) tube. The opening of nanotube sidewall can be clearly seen. The details of the geometry parameters are given in table 7.

Table 7. Geometrical variables (A—B: bond length in unit of Å, A—B—C: bond angle in unit of degree) of a CH_2 attached nine-layered (6,6) finite tube from EHTB and GGA calculations. The large C2—C3 distance indicates opening of nanotube sidewall by CH_2 functionalization.

Variable	*EHTB*	*GGA*
C1—H1	1.09	1.11
C1—C2	1.53	1.45
C2—C3	2.28	2.13
C3—C4	1.40	1.42
C4—C5	2.45	2.46
H1—C1—H2	112.83	107.97
C2—C1—C3	96.2	95.18
C4—C3—C1	117.67	118.06
C4—C3—C5	123.08	120.75

5. Conclusions

In summary, we have constructed a nonorthogonal tight-binding total energy model for hydrocarbons in spirit of extended Hückel theory. Test calculations on a variety of molecules and nanostructures have been performed. The satisfactory performance on structural parameters, binding energies, vibration frequencies and charge transfer on hydrocarbon molecules prove the validity and transferability of our EHTB model. It also reproduces the size-dependent binding energy of carbon fullerenes and nanotubes, formation energy of defect, Young's modulus and structural change by chemical functionalization from GGA calculations. Therefore, EHTB model could be a promising tool in the simulations of hydrocarbon molecules and carbon nanostructures (e.g. fullerenes, nanodiamond, nanotubes) up to relatively larger sizes and longer time scale, for which *ab initio* methods are limited by its computational cost.

Acknowledgements

We acknowledge supports from the Office of Naval Research (USA) under Grant N00014-01-1-0802, the Department of Energy (USA) under Grant DEFG0397 SF21388, the NCET Program provided by the Ministry of Education of China, the National Natural Science Foundation of China (50402025, 50234020, 10472022).

References

[1] K. Ohno, K. Esfarjani, Y. Kawazoe. *Computational Materials Science*, Springer, Berlin (1999).
[2] M.C. Payne, M.T. Teter, D.C. Allen, T.A. Arias, J.D. Joannopoulos. Iterative minimization techniques for *ab initio* total-energy calculations: molecular dynamics and conjugate gradients. *Rev. Mod. Phys.*, **64**, 1045 (1992).
[3] A.K. Rappe, C.J. Casewit, K.S. Colwell, W.A. Goddard III, W.M. Skiff. UFF, a full periodic table force field for molecular mechanics and molecular dynamics simulations. *J. Am. Chem. Soc.*, **114**, 10024 (1992).
[4] J. Tersoff. Modeling solid-state chemistry: interatomic potentials for multicomponent systems. *Phys. Rev. B*, **39**, 5566 (1989).
[5] D.W. Brenner. Empirical potential for hydrocarbons for use in simulating the chemical vapor deposition of diamond films. *Phys. Rev. B*, **42**, 9458 (1990).
[6] S. Goedcker. Linear scaling electronic structure methods. *Rev. Mod. Phys.*, **71**, 1085 (1999).
[7] S.Y. Wu, C.S. Jayanthi. Order-*N* methodologies and their applications. *Phys. Rep.*, **358**, 1 (2002).
[8] D.J. Chadi. Atomic and electronic structures of reconstructed Si(100) surfaces. *Phys. Rev. Lett.*, **43**, 43 (1979).
[9] P.C. Slater, G.F. Koster. Simplified LCAO method for the periodic potential problem. *Phys. Rev.*, **94**, 1498 (1954).
[10] C.Z. Wang, K.M. Ho. Tight-binding molecular dynamics studies of covalent systems. In *Advances in Chemical Physics*, I. Prigogine, S.A. Rice (Eds.), Vol. XCIII, p. 651, John Wiley & Sones, Inc., New York (1996).
[11] C.M. Goringe, D.R. Bowler, E. Herhandez. Tight-binding modelling of materials. *Rep. Prog. Phys.*, **60**, 1447 (1997).
[12] M.J. Mehl, D.A. Papaconstantopoulos. Tight-binding parameterization of first-principles results, Chapter V. In *Topics in Computational Materials Science*, C.Y. Fong (Ed.), p. 169, World Scientific, Singapore (1998).

[13] J.J. Zhao, J.L. Wang, G.H. Wang. A transferable nonorthogonal tight-binding model of germanium: application to small clusters. *Phys. Lett. A*, **275**, 281 (2000).
[14] B.N. Davidson, W.E. Pickett. Tight-binding study of hydrogen on the C(111), C(100), and C(110) diamond surfaces. *Phys. Rev. B*, **49**, 11253 (1994).
[15] Y. Wang, C.H. Mak. Transferable tight-bonding potential for hydrocarbons. *Chem. Phys. Lett.*, **235**, 37 (1995).
[16] A.P. Horsfield, P.D. Godwin, D.G. Pettifor, A.P. Sutton. Computational materials synthesis. I. A tight-binding scheme for hydrocarbons. *Phys. Rev. B*, **54**, 15773 (1996).
[17] M.D. Winn, M. Rassinger, J. Haffner. Tight-binding potential for hydrocarbons. *Phys. Rev. B*, **55**, 5364 (1997).
[18] B.C. Pan. Tight-binding potential for hydrocarbons. *Phys. Rev. B*, **64**, 155408 (2001).
[19] R. Hoffmann. An extended Hckel theory. I. Hydrocarbons. *J. Chem. Phys.*, **39**, 1397 (1963).
[20] G. Calzaferri, L. Forss, I. Kamber. Molecular geometries by the extended Hueckel molecular orbital (EHMO) method. *J. Phys. Chem.*, **93**, 5366 (1989).
[21] E. Curotto, A. Matro, D. Freeman, J.D. Doll. A semi-empirical potential for simulations of transition metal clusters: minima and isomers of Ni_n ($n = 2–13$) and their hydrides. *J. Chem. Phys.*, **108**, 729 (1998).
[22] M. Brändle, G. Calzaferri. Molecular geometries by the extended-Hückel molecular orbital method II: hydrocarbons and organic molecules containing O, N, and S. *Helv. Chim. Acta*, **76**, 924 (1993).
[23] W. Harrison. *Electronic Structures and the Properties of Solids*, Freeman, San Francisco (1980).
[24] D. Lu, J. Nocedal. On the limited memory BFGS method for large scale optimization. *Math. Program. B*, **45**, 503 (1989).
[25] J. Andzelm, E. Wimmer. Density functional Gaussian-type-orbital approach to molecular geometries, vibrations, and reaction energies. *J. Chem. Phys.*, **96**, 1280 (1992) and references therein.
[26] W.J. Hehre, L. Radom, P. Schleyer, J.A. Pople. Ab Initio *Molecular Orbital Theory*, Wiley, New York (1986).
[27] A. Almenningen, T. Jonvik, H.D. Martin, T. Urbanek. Cubane molecular structure determined by gas-phase electron diffraction. *J. Mol. Struct.*, **128**, 239 (1985).
[28] M.W. Schmidt, K.K. Baldridge, J.A. Boatz, S.T. Elbert, M.S. Gordon, J.H. Jensen, S. Koseki, N. Matsunaga, K.A. Nguyen, S.J. Su, T.L. Windus, M. Dupuis, J.A. Montgomery. General atomic and molecular electronic structure system. *J. Comput. Chem.*, **14**, 1347 (1993).
[29] B. Delley. An all-electron numerical method for solving the local density functional for polyatomic molecules. *J. Chem. Phys.*, **92**, 508 (1990); B. Delley, From molecules to solids with the $DMol^3$ approach, *J. Chem. Phys.* **113**, 7756 (2000).
[30] J.P. Perdew, Y. Wang. Accurate and simple analytic representation of the electron–gas correlation energy. *Phys. Rev. B*, **45**, 13244 (1992).
[31] R. Saito, G. Dresslehaus, M.S. Dresselhaus. *Physical Properties of Carbon Nanotubes*, Imperial College Press, London (1998).
[32] J.J. Zhao, B. Wen, Z. Zhou, Z.F. Chen, P.R. Schleyer. Reduced Li diffusion barriers in composite BC_3 nanotubes. *Chem. Phys. Lett.*, **415**, 323 (2005).
[33] N. Chandra, S. Namilae, C. Shet. Local elastic properties of carbon nanotubes in the presence of Stone–Wales defects. *Phys. Rev. B*, **69**, 094101 (2004), and references therein.
[34] G.V. Lier, C.V. Alsenoy, V.V. Doren, P. Geerlings. *Ab initio* study of the elastic properties of single-walled carbon nanotubes and graphene. *Chem. Phys. Lett.*, **326**, 181 (2000).
[35] Z. Chen, S. Nagase, A. Hirsch, R.C. Haddon, W. Thiel, P.von R. Schleyer. Side-wall opening of single-walled carbon nanotubes (SWCNTs) by chemical modification: a critical theoretical study. *Angew. Chem. Int. Ed.*, **43** (2004).
[36] J.J. Zhao, Z.F. Chen, Z. Zhou, H. Park, P.R. Schleyer, J.P. Lu. Engineering the electronic structure of single-walled carbon nanotubes by chemical functionalization. *Chem. Phys. Chem.*, **6**, 598 (2005).
[37] Z. Chen, H. Jiao, M. Búhl, A. Hirsch, W. Thiel. Theoretical investigation into structures and magnetic properties of smaller fullerenes and their heteroanalogues. *Theor. Chem. Acc.*, **106**, 352 (2001).
[38] Z. Chen, J. Cioslowski, N. Rao, D. Moncrieff, M. Bühl, A. Hirsch, W. Thiel. Endohedral chemical shifts in higher fullerenes with 72–86 carbon atoms. *Theor. Chem. Acc.*, **106**, 364 (2001).
[39] Z. Chen, W. Thiel. Performance of semiempirical methods in fullerene chemistry: relative energies and nucleus-independent chemical shifts. *Chem. Phys. Lett.*, **367**, 15 (2003).
[40] G. Zheng, S. Irle, K. Morokuma. Performance of the DFTB method in comparison to DFT and semiempirical methods for geometries and energies of C20CC86 fullerene isomers. *Chem. Phys. Lett.*, **412**, 210 (2005).